Supplementary Information

Microplastics encapsulation in aragonite: efficiency, detection and insight into potential environmental impacts

Nives Matijaković Mlinarić[a], Katarina Marušić[a], Antun Lovro Brkić[b], Marijan Marciuš[a], Tamara Aleksandrov Fabijanić[d], Nenad Tomašić[c], Atiđa Selmani[e], Eva Roblegg[e], Damir Kralj[a], Ivana Stanić[a], Branka Njegić Džakula[a]*, Jasminka Kontrec[a]*

[a]Division of Materials Chemistry, Ruđer Bošković Institute, Bijenička cesta 54, 10000 Zagreb, Croatia
[b]Institute of Physics, Bijenička cesta 46, 10000 Zagreb, Croatia
[c]Department of Geology, Faculty of Science, University of Zagreb, Horvatovac 102a, Zagreb, Croatia
[d]The Faculty of Mechanical Engineering and Naval Architecture, University of Zagreb, Ivana Lučića 5, 10000 Zagreb, Croatia
[e]Pharmaceutical Technology and Biopharmacy, Institute of Pharmaceutical Sciences, University of Graz, Universitatsplatz 1, 8010 Graz, Austria
*Correspondence: jasminka.kontrec@irb.hr (J. K.); bnjeg@irb.hr (B. Nj. Dž.) Tel. +385 1 456 1004

The Supplementary Information contains detailed experimental procedures and analyses, Table SI1. (Solution composition of prepared artificial seawater, ASW), Table SI2 (The results of measured mechanical properties), and the following figures: scanning electron microscopy (SEM) image of aragonite samples in the reference system and the system with untreated and HA-treated PE and PS (Figure SI1), washed samples prepared in the presence of PS and PE microspheres (Figure SI2), chloroform washed sample prepared in the presence of PS microspheres-thickness of aragonite layer around the encapsulated microsphere (Figure SI3), particle size distribution of polyethylene (PE) microparticles (Figure SI4).

Experimental

Table SI1. Solution composition of prepared artificial seawater (ASW) which mimics the ionic composition of typical seawater or extrapallial solution of marine and freshwater species (Tracy et al., 1998)

ion	c / mmol dm^{-3}
Ca^{2+}	10
Mg^{2+}	50
Na^{+}	470
Cl^{-}	540
CO_3^{2-}	5
SO_4^{2-}	30
K^{+}	10

Tracy, S.L., Francois, C.J.P., Jennings, H.., 1998. The growth of calcite spherulites from solution. J. Cryst. Growth 193, 374–381. https://doi.org/10.1016/s0022-0248(98)00521-1

Calcium carbonate precipitation

Calculations of molar concentrations and activities of the relevant ionic species and supersaturation were performed using an algorithm developed in our laboratory. They were comparable to calculations performed using VMINTEQ 3.0 (available at http://vminteq.lwr.kth.se/download/). The solution supersaturation was expressed as the aragonite saturation ratio, S_A, and was defined as the square root of the quotient of the ion activity product, $a(Ca^{2+}) \times a(CO_3^{2-})$, and the thermodynamic solubility product of aragonite, K_{sp}^0: $S_A = [(a(Ca^{2+}) \times a(CO_3^{2-}))/K_{sp}^0]^{1/2}$. The modified Debye-Hückel equation, proposed by Davies, was used to calculate the activity coefficients of the z-valent ions, y_z (Davis, 1962). The equations for the charge and mass balance as well as the respective protolytic equilibria and the equilibrium constants used, have been described in our previous publications (Kralj et al., 1997, 1994, 1990; Njegić-Džakula et al., 2009).

Contact angle and colour measurements

The instrument was programmed with the following settings: measurement geometry d/8° (diffuse illumination, 8-degree viewing), selecting an area of 3 mm in diameter (SAV, Small Average Value), CIE Standard Illuminant D65 corresponding to the average daylight, CIE 1964 Standard Observer (10° standard observer). The spectrophotometer was set to take four consecutive measurements at each point, which gave the mean value of the colour coordinates. The measurements were performed simultaneously using the Specular Component Included (SCI) and Specular Component Excluded (SCE) methods. However, since no significant difference was found between the data, only the results obtained with the SCI method are presented in the manuscript. The change in colour characteristics of the samples PS and PE upon adsorption of HA on the surface was studied using CIE colourimetry in the CIELAB system (Marušić et al., 2022, 2020). In the CIELAB colour space, L^* indicates lightness on a scale from 0 (black) to 100 (white). In contrast, the chromaticity of a colour is represented in a two-dimensional diagram in which the a* axis determines the ratio of green (negative) to red (positive). The *b** axis determines the blue (negative) to yellow (positive) ratio. The measure used to evaluate the total colour change is the CIE 1976 *L*a*b** colour difference, which is simply calculated as the Euclidean distance in CIELAB space. For colours specified by the parameters [L_1*, a_1*, b_1*] and [L_2*, a_2*, b_2*], the difference, ΔE^*_{ab}, is calculated as follows:

$$\Delta Eab^* = \sqrt{(L_1^* - L_2^*)^2 + (a_1^* - a_2^*)^2 + (b_1^* - b_2^*)^2}$$

Results

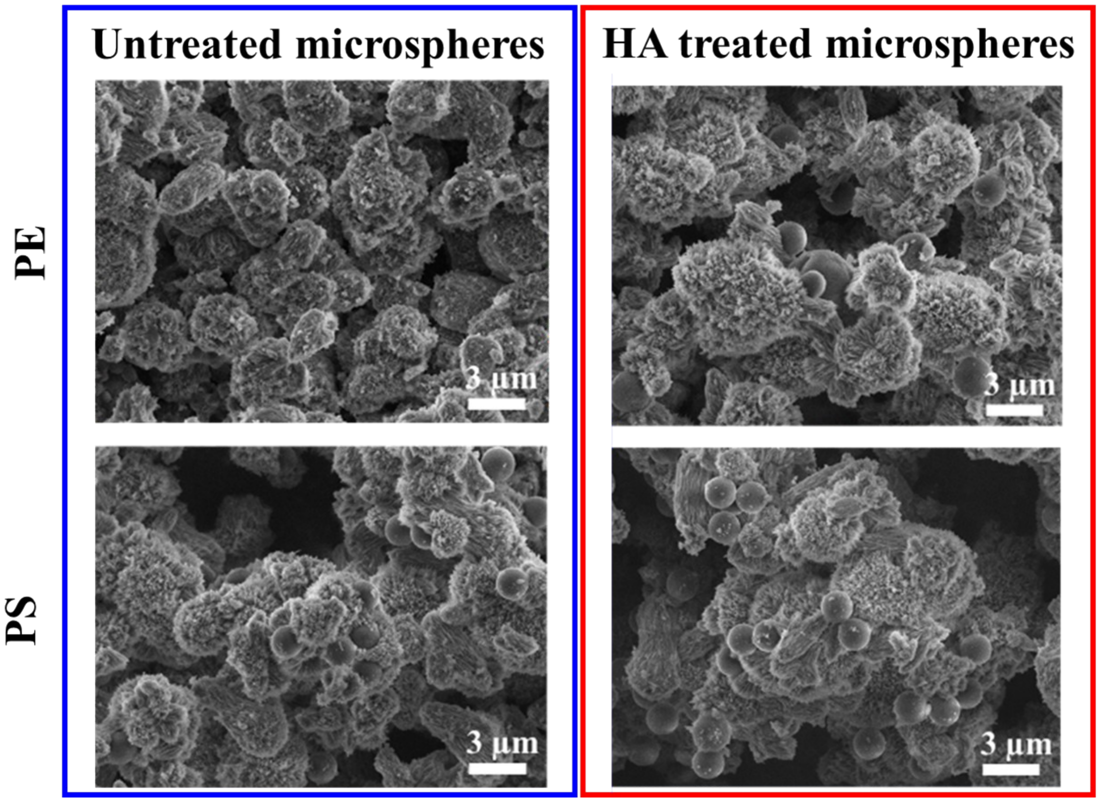

Figure SI1. SEM images of aragonite samples in the system with untreated and HA-treated PE and PS

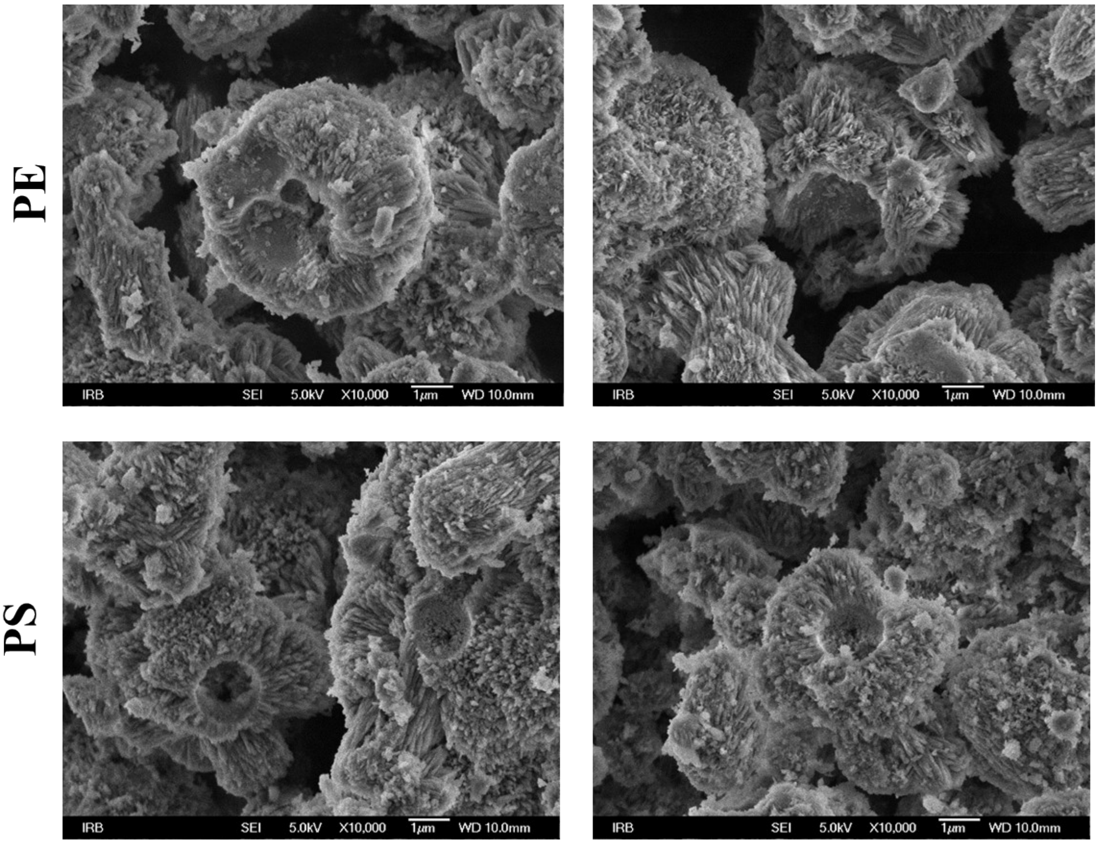

Figure SI2. SEM image of washed samples prepared in the presence of PS and PE microspheres.

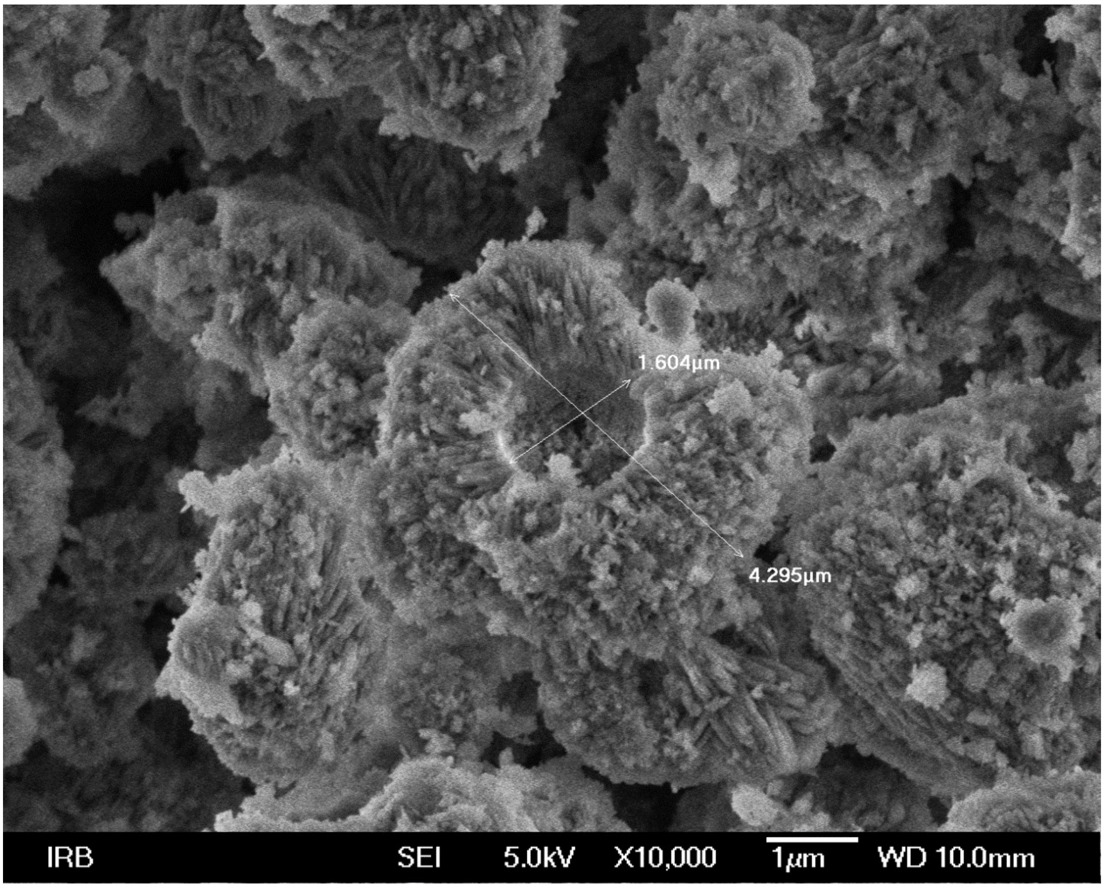

Figure SI3. SEM image of chloroform washed sample prepared in the presence of PS microspheres-thickness of aragonite layer around the encapsulated microsphere.

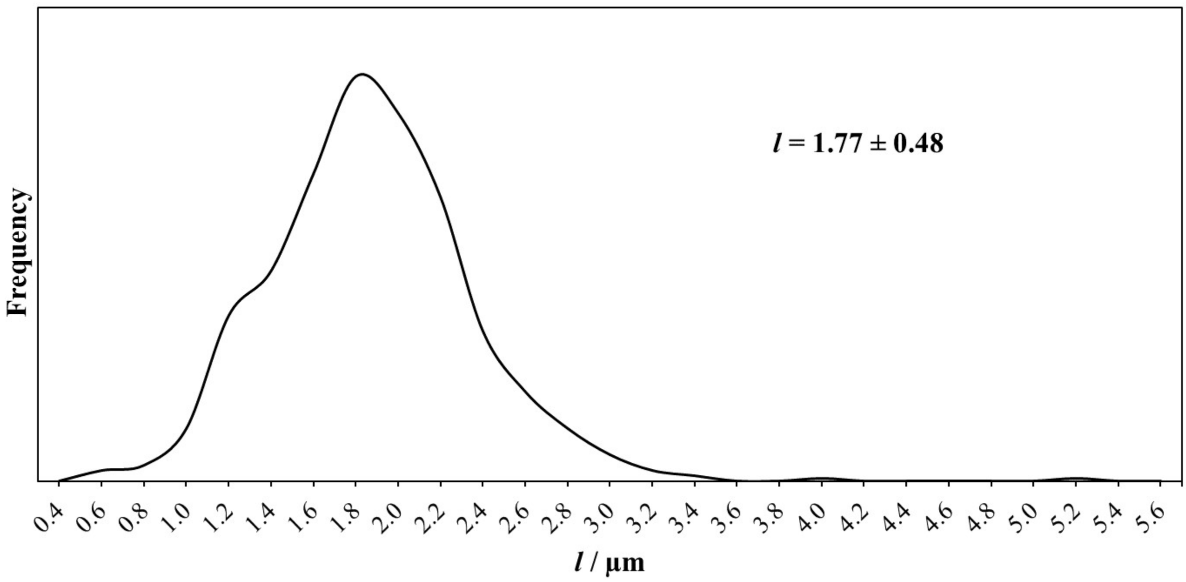

Figure SI4. Particle size distribution of PE microparticles. The size distribution was determined by analyzing approximately 1000 particles from SEM images.

Instrumented Indentation Test (IIT)

The mechanical properties of the samples (pure aragonite and aragonite with encapsulated PS-HA and PE-HA) were determined by continuously recording the force and the depth of indentation at a loading and unloading rate of 6000 mN/min. The test force, *F*, the corresponding indentation depth, *h*, and time were recorded during the test procedure [EN ISO 14577-1:2015]. A Poisson's ratio of 0.3 was assumed for all samples.

Instrumented indentation test IIT results were obtained using the Olivier & Parr method. The indentation plane strain modulus (E^*), indentation modulus (E_{IT}), indentation hardness (H_{IT}), Vickers instrumented hardness (HV_{IT}), stiffness (S), elastic work (W_{elast}), plastic work (W_{plast}), indentation work ratio (η_{IT}), and indentation creep (C_{IT}) were determined. The results of the measured mechanical properties are presented in Table SI1.

Table SI2. The results of measured mechanical properties of pure aragonite and aragonite samples with encapsulated microspheres treated with humic acid: polystyrene (PS-HA) and polyethylene (PE-HA).

Pure aragonite									
	E*, **GPa**	E_{IT}, **GPa**	H_{IT}, **MPa**	HV_{IT} **(HV)**	***S*****, mN/nm**	W_{elast}, **pJ**	W_{plast}, **pJ**	η_{IT}, **%**	C_{IT}, **%**
Min	33.8	30.8	452.7	42.7	1.693	450603	3030812	12.4	4.807
Max	34.9	31.8	505.7	47.7	1.766	468202	3190451	13.1	5.629
Mean	**34.3**	**31.2**	**481.3**	**45.4**	**1.736**	**457264**	**3122042**	**12.8**	**5.096**
St dev	0.4	0.4	16.8	1.58	0.022	5499	53402	0.2	0.259
PS-HA									
	E*, **GPa**	E_{IT}, **GPa**	H_{IT}, **MPa**	HV_{IT} **(HV)**	***S*****, mN/nm**	W_{elast}, **pJ**	W_{plast}, **pJ**	η_{IT}, **%**	C_{IT}, **%**
Min	24.3	22.1	325.9	30.8	1.485	517875	3643704	12.0	4.600
Max	25.9	23.6	361.0	34.1	1.551	530793	3818420	12.7	5.299
Mean	**24.9**	**22.6**	**336.2**	**31.7**	**1.517**	**525014**	**3705571**	**12.4**	**4.858**
St dev	0.6	0.5	10.5	1.0	0.021	3958	62786	0.2	0.216
PE-HA									
	E**, GPa**	E_{IT}, **GPa**	H_{IT}, **MPa**	HV_{IT} **(HV)**	***S*****, mN/nm**	W_{elast}, **pJ**	W_{plast}, **pJ**	η_{IT}, **%**	C_{IT}, **%**
Min	11.7	10.6	256.3	24.2	0.803	1004451	3996030	19.8	7.719
Max	15.1	13.8	309.0	29.2	1.065	1058232	4273330	20.2	8.345
Mean	**12.7**	**11.5**	**286.1**	**27.0**	**0.848**	**1031573**	**4127137**	**20.0**	**8.073**
St dev	1.3	1.1	20.9	2.0	0.106	22602	124187	0.2	0.278

References:

Davis CW (1962) Ion Association. Butterworths, London

Kralj D, Brečević L, Kontrec J (1997) Vaterite growth and dissolution in aqueous solution III. Kinetics of transformation. J Cryst Growth 177:248–257. https://doi.org/10.1016/S0022-0248(96)01128-1

Kralj D, Brečević L, Nielsen AE (1990) Vaterite growth and dissolution in aqueous solution I. Kinetics of crystal growth. J Cryst Growth 104:793–800. https://doi.org/10.1016/0022-0248(90)90104-S

Kralj D, Brečević L, Nielsen AE (1994) Vaterite growth and dissolution in aqueous solution II. Kinetics of dissolution. J Cryst Growth 143:269–276. https://doi.org/10.1016/0022-0248(94)90067-1

Njegić-Džakula B, Brečević L, Falini G, Kralj D (2009) Calcite Crystal Growth Kinetics in the Presence of Charged Synthetic Polypeptides. Cryst Growth Des 9:2425–2434. https://doi.org/10.1021/cg801338b